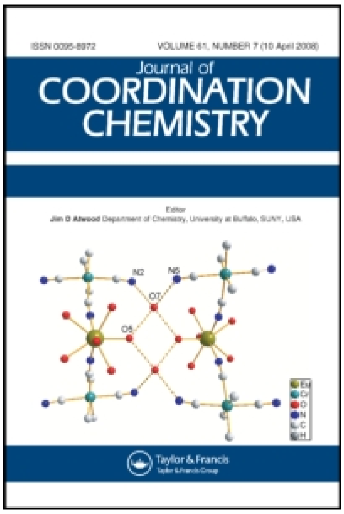

Journal of Coordination Chemistry
Publication details, including instructions for authors and subscription information:
http://www.informaworld.com/smpp/title~content=t713455674

Supramolecular structural and spectral perspectives of novel ruthenium(III) azodye complexes

Ahmed T. Mubarak[a]; A. Z. El-Sonbati[a]; S. M. Ahmed[a]
[a] Faculty of Science, Department of Chemistry, King Khalid University, Abha 61413, Saudi Arabia

To cite this Article Mubarak, Ahmed T. , El-Sonbati, A. Z. and Ahmed, S. M.(2007) 'Supramolecular structural and spectral perspectives of novel ruthenium(III) azodye complexes', Journal of Coordination Chemistry, 60: 17, 1877 — 1890
To link to this Article: DOI: 10.1080/00958970701203123
URL: http://dx.doi.org/10.1080/00958970701203123

Journal of Coordination Chemistry
Vol. 60, No. 17, September 2007, 1877–1890

Supramolecular structural and spectral perspectives of novel ruthenium(III) azodye complexes

AHMED T. MUBARAK*, A. Z. EL-SONBATI and S. M. AHMED

Faculty of Science, Department of Chemistry, King Khalid University,
P.O. Box 9004, Abha 61413, Saudi Arabia

(*Received 17 September 2006; revised 8 November 2006; in final form 10 November 2006*)

Five *bis*-[5-(4′-*R*-phenylazo)-8-hydroxyquinoline] ruthenium complexes [$\mathrm{RuLn \cdot Cl_2 \cdot OH_2}$]; where Ln = 5-(4′-*R*-phenylazo)-8-hydroxyquinolinol, $R = \mathrm{OCH_3}$ ($n = 1$), $\mathrm{CH_3}$(2), H(3), Cl(4), $\mathrm{NO_2}$(5), have been prepared and characterized on the basis of elemental analyses, IR, ^{1}H NMR, ESR, thermal analysis and magnetic susceptibility measurements. The data show that these complexes exist in trans-isomeric solid form. Two inversion-related ligands and two $\mathrm{Ru^{3+}}$ atoms form a cage-like dimer. Both ligands of the dimer are bridged by a pair of inversion-related Ru–N (azodye) bonds. The octahedral coordination geometry of $\mathrm{Ru^{3+}}$ is made up of an N of pyridine, the deprotonated quinoline O atom, one of the azodye N atoms, two chlorides and one water. The ligands in the dimer are stacked over one another. In the solid state of azo-8-hydroxyquinoline, the dimers have inter-and intramolecular hydrogen bonds. Interactions between the ligands and the metal are discussed. The azo group was involved in chelation for all the prepared complexes. The effect of Hammet's constant on the ligand field parameters are also discussed and drawn.

Keywords: Supramolecular structures; Azoquinoline complexes; Hydrogen bonded systems; Ligand field parameters

1. Introduction

Hydrogen bonding plays an important role in biology, allowing the reversible formation of the non-covalently linked to aggregate. Base pairing in DNA is only possible due to complementary binding sites of the nucleobases guanine, cytosine, thymine and adenine. Jørgensen [1] found that the stability of multiple hydrogen bonded ‘‘dimer’’ depends not only on the number of hydrogen bonds but also on the hydrogen bonding pattern.

Our interest in the supramolecular chemistry of 8-hydroxyquinoline derivatives arises from their versatility [2–4] as well as the hydrogen bonding ability of these molecules [5]. In an ongoing project we are studying *bis*-[5-(4′-*R*-phenylazo)-8-hydroxyquinoline] for formation of hydrogen bonded polymer complexes in the solid state [2].

---

*Corresponding author. Email: atmubarak@kku.edu.sa

Journal of Coordination Chemistry
ISSN 0095-8972 print/ISSN 1029-0389 online © 2007 Taylor & Francis
DOI: 10.1080/00958970701203123

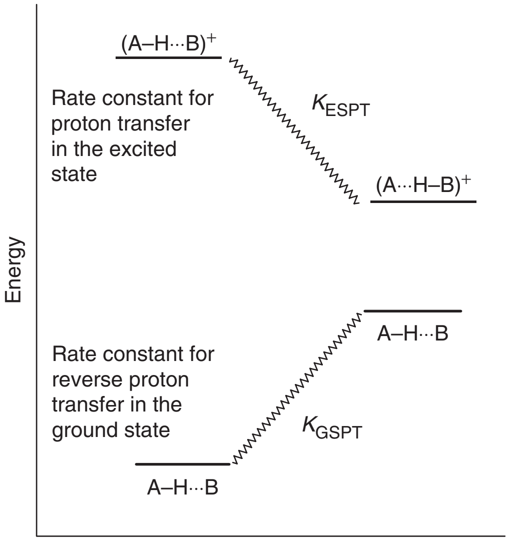

Figure 1. A four-state proton transfer cycle.

The chemistry of quinoline and its derivatives has also attracted special interest due to their therapeutic properties [6]. Quinoline sulphonamides have been used in treatment of cancer [7], turberculosis [8], diabetes [9], malaria [10] and convulsion [11].

Proton transfer reactions are important in chemistry. In biological systems, the transport of protons through membrane proteins stores energy for the synthesis of biomolecules [12]. Proton transfer reactions are also the basis of acid-base chemistry and are important to the structure and dynamics of hydrogen bonds. Excited-state proton transfer reactions are useful models for studying proton transfer. The simplest four-state proton transfer cycle, shown in figure 1, begins with photoexcitation of a hydrogen-bonded complex to an excited electronic state that has a very different acidity from the ground electronic state [13]. This excited species rapidly transfers the proton across the hydrogen bond.

A number of recent papers from the laboratory of Mubarak, El-Sonbati and co-workers [14–26], have described the preparation and isolation of novel supramolecular solid complexes of several sterically hindered heterocyclic ligands, namely 1-phenyl-3-methyl-(4-derivatives phenylhydrazo)-5-pyrazolone, 8-hydroxy-7-quinolinecarboxaldehyde, quinoline Schiff bases, *bis*[5-(2-carboxyphenyldiazo)-8-hydroxy-7 -quinolinecarboxaldehyde, *bis*[5-(2-hydroxyphenyldiazo)-8-hydroxy-7-quinolinecarboxaldehyde], poly[N-(2$^-$-pyridyl)propenamide], allylazo-β-diketone, N-acryloyl-1-phenyl-2-thiourea. El-Sonbati and Mubarak were the first who prepared 5-(4′-derivatives phenyldiazo)-8-hydroxy quinoline, but they have not isolated its solid complexes with metal halides in various oxidation states. Azo compounds are used in analytical separation of metal ions in mixtures as analytical reagents [15–19], in new structural features of the coordination complexes and have biological activity [20–22]. A literature survey indicates, however, little research on the synthesis and properties of these materials.

In this article, we describe the synthesis of a series of 8-hydroxyquinoline azodye derivatives as additional hydrogen bond donor/acceptor moieties in the 8-position. The interest is focused on studying the chelating properties of 8-hydroxyquinoline and its azo compounds based on elemental analysis, magnetic moments and spectral methods (UV–Vis, IR). In the future, we will examine hydrogen bond donor/acceptor moieties in the 5-and/or 7-position of the quinoline structure.

2. Experimental

2.1. *Synthesis of the ligand*

The standard chemicals 8-hydroxyquinoline, aniline and 4-alkylanilines (alkyl: OCH_3, CH_3, Cl and NO_2; Aldrich Chemical Co.) have been used without further purification.

2.2. *Preparation of 5-phenylazo-8-hydroxyquinoline (HL_3)*

In a typical preparation, 25 mL of distilled water containing hydrochloric acid (12 M, 2.68 mL, 32.19 mmol) was added to aniline (0.979 mL, 10.73 mmol). To the resulting mixture stirred and cooled to 0°C, a solution of sodium nitrite (740 mg, 10.73 mmol, in 20 mL of water) was added dropwise. The so-formed diazoium chloride was consecutively coupled with an alkaline solution of 8-hydroxyquinoline (1.557 g, 10.73 mmol) in 20 mL of ethanol containing 602 mg (10.73 mmol) of potassium hydroxide. The orange precipitate formed was immediately filtered and washed several times with distilled water. The crude product was then purified by recrystallization from hot ethanol in 65–75% yield. The obtained analytical data confirmed the expected composition, table 1. The ligands were also characterized by ^{1}H NMR and IR spectroscopy.

2.3. *Preparation of the metal complexes*

All the metal azodye complexes in this work were prepared through direct interaction of $RuCl_3 \cdot 3H_2O$ with the azodye. The ligand (0.01 mol) was suspended in ethanol and refluxed for 15 min. Ethanolic solution of metal salts (0.01 mol) was added slowly to the stirred ligand and the reaction mixture was further refluxed. The coloured precipitates were filtered through a sintered glass crucible and washed several times with ethanol, ether and finally dried in a vacuum desiccator for 24 h to give the complexes as powders. The analytical results for *bis*-azodye compounds are reported in table 1.

2.4. *Measurements*

Microanalyses of all samples were carried out at King Khalid University Analytical Center, Saudi Arabia, using a Perkin–Elmer 2400 Series II Analyzer. The metal content in the complexes was estimated by standard methods [22–26]. IR spectra were recorded on a Perkin–Elmer 1340 spectrophotometer. UV–Vis Spectra were measured (Nujol mull) on a Pye Unicam 8800 spectrophotometer. Magnetic measurements were carried out at room temperature using Gouy's method, employing $Hg[Co(SCN)_4]$ for calibration, and were corrected for diamagnetism by using Pascal's constants. Magnetic moments were calculated using the equation: $\mu_{\mathrm{eff}} = 2.84\ [T\chi_{\mathrm{M}}^{\mathrm{corr}}]^{1/2}$.

Table 1. Analytical data for Ru^{3+} complexes[a] of *bis*-[5-(4′-*R*-phenylazo)-8-hydroxyquinoline] (HL_n) for molecular structure see figure 5).[b]

Complex[c]	Code	Yield (%)	Exp. (Calcd)% C	H	N
HL_1			69.0 (68.8)	4.8 (4.7)	15.4 (15.1)
$[Ru(L_1)Cl_2 \cdot OH_2]_2$	1	89	39.8 (40.0)	3.1 (3.0)	9.3 (8.9)
HL_2			73.2 (73.0)	5.1 (5.0)	16.3 (16.0)
$[Ru(L_2)Cl_2 \cdot OH_2]_2$	2	82	41.4 (41.6)	2.9 (3.1)	9.5 (9.1)
HL_3			72.2 (72.3)	4.4 (4.5)	16.6 (16.9)
$[Ru(L_3)Cl_2 \cdot OH_2]_2$	3	77	40.2 (40.2)	2.5 (2.7)	9.7 (9.4)
HL_4			63.4 (63.5)	3.4 (3.6)	14.7 (14.8)
$[Ru(L_4)Cl_2 \cdot OH_2]_2$	4	70	37.1 (37.3)	2.2 (2.3)	9.0 (8.7)
HL_5			61.1 (61.2)	3.5 (3.4)	19.4 (19.1)
$[Ru(L_5)Cl_2 \cdot OH_2]_2$	5	65	37.1 (37.3)	2.1 (2.3)	13.0 (13.3)

[a] Microanalytical data as well as metal estimations are in good agreement with the stoichiometry of the proposed complexes.
[b] The excellent agreement between calculated and experimental data supports the assignment suggested in the present work.
[c] L_1–L_5 are the anions of the ligands HL_1–HL_5 as given in figure 5.

The ^1H and ^{13}C NMR spectra were obtained on a JEOL FX 900 Q Fourier transform spectrometer with DMSO-d_6 as solvent and TMS as internal reference. TG measurements were made using a DuPont 950 thermo balance. Ten milligram samples were heated at $10^\circ\,min^{-1}$ in a dynamic nitrogen atmosphere ($70\,mL\,min^{-1}$); the sample holder was boat-shaped, $10 \times 5 \times 2.5\,mm^3$ deep; the temperature measuring thermocouple was placed within 1 mm of the holder. The halogen content was determined by combustion of the solid complex (30 mg) in an oxygen flask in the presence of a KOH–H_2O_2 mixture. The halide content was then determined by titration with a standard $Hg(NO_3)_2$ solution using diphenyl carbazone as an indicator.

3. Results and discussion

3.1. *Bonding atoms and stereochemistry*

3.1.1. General remarks. The transfer of two equivalent protons within a doubly hydrogen-bonded dimer is an important type of excited-state proton transfer. The two molecules of 8-hydroxyquinoline, form, in solution, doubly hydrogen-bonded dimers from excited-state double proton transfer. Figure 2 shows the structures of both the dimer and the tautomer.

Mubarak, El-Sonbati, Bardez and coworkers [2, 15, 17, 18, 20, 27] have characterized the steady-state spectroscopy of 8-hydroxyquinoline which forms a very stable

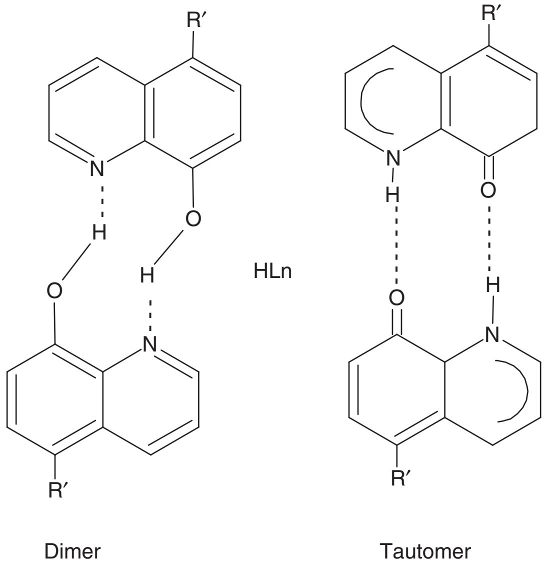

Figure 2. Structure of the dimer and tautomer of 8-hydroxyquinoline.

hydrogen-bonded dimer whose structure is given in figure 2 along with that for the tautomer. The infrared spectrum of the O–H stretching transition of the dimers indicates tremendous stability. Although the vibrational spectra of hydrogen-bonded molecules are often very broad, the O–H stretching transition of 8-hydroxyquinoline dimers has a width of only about $25\,\mathrm{cm}^{-1}$, indicating that the dimers are well-defined with stable structures. Typically, aromatic systems that form hydrogen-bonded dimers in the ground state show a new features corresponding to the dimer and an associated isosbestic point as a function of concentration. These features do not appear in the 8-hydroxyquinoline spectra because, even at very low concentration, dimers are the dominant species.

3.2. *The solid state structures of azodye-8-hydroxyquinolinol*

The two hydroxyquinoline units (figure 3) lie in one plane with intermolecular (**I**) and intramolecular (**II**) hydrogen bonding between the hydroxyl group and the quinoline nitrogen atom. The intermolecular hydrogen bond distance is shorter than the intramolecular distance, as reported for other 8-hydroxyquinoline dimers [2, 3, 5]. This might arise from an unfavorable small O–H–N angle of the intramolecular interaction [5] as the additional H-bond influences the hydrogen bonding ability of the hydrogen by electronic and/or steric factors. The overall structure of the dimer is close to planar with a slight shift of the two quioline units from the plane.

Hydroxyquinoline shows a monomer dimer equilibrium in solution [28, 29]. A strong intramolecular hydrogen bond is present in the monomer [2, 30] and two such monomers form a dimer with additional hydrogen bonding yielding the bifurcated hydrogen bonds and H–N–H nitrogen bridges (figure 3). The dimer is able to dissociate, while the intramolecular interaction can only be broken if appropriate hydrogen

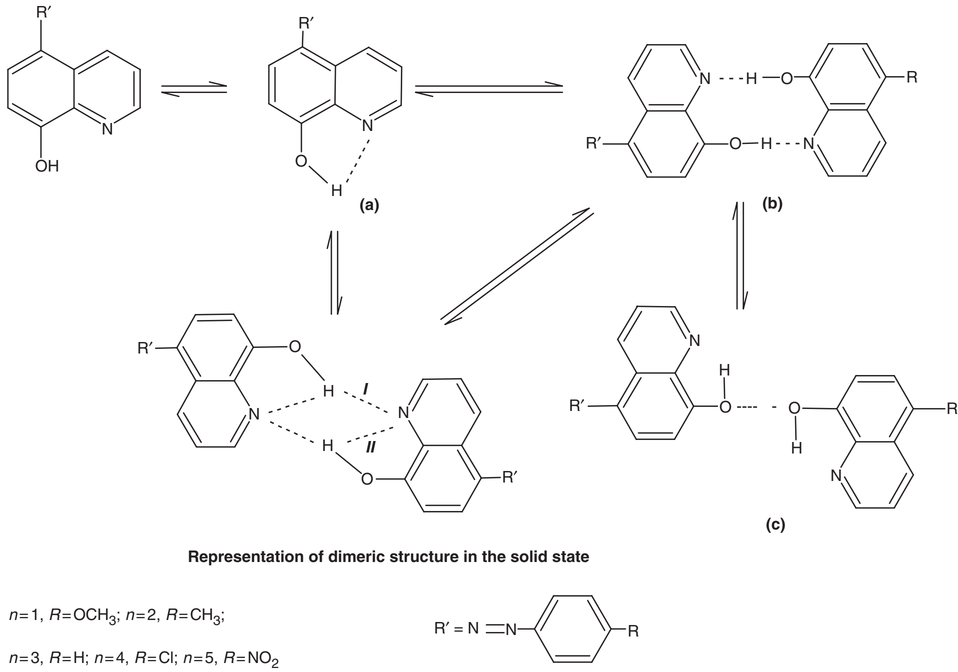

Figure 3. General formula and proton numbering of 5-(4′-*R*-phenylazo)-8-hydroxyquinolinol (HL_n).

bond acceptors are attached and then act as competitors to the quinoline nitrogen atoms [4].

Most of the azo compounds give spectral bands in the wavelength range 46,620–34,480 and 31,250–270,370 cm^{-1}. The former region is due to the absorption of the aromatic ring compared to ^1B_b and ^1L_b of mono substituted benzene; while the latter is due to conjugation between the azo group and the aromatic nuclei with intermolecular charge transfer resulting from π-electron migration to the diazo group from electron donating substituents. The *p*-substituents increase the conjugation with a shift to a longer wavelength. Most of the simple *p*-substituted compounds are in the azoid form in cyclohexane and alcohols. The substituent effect is related to Hammet's constants [31]. The position of the π–π^* transition of the azo groups is an ambiguous and intriguing phenomenon in molecular spectroscopy. For azo benzenes, as the possibilities of the mesomerism became greater, the stabilization of the excited state is increased relative to that of the ground state and a bathochromic shift of the absorption bands follow [32]. Based on MO theory the energy terms of the molecular orbital became more closely spaced as the size of the conjugated system increases [32]. Therefore, with every additional conjugated double bond the energy difference between the highest occupied and the lowest vacant π-electron levels became smaller and the wavelength of the first absorption band corresponding to this transition increases. The azo group acts as a proton acceptor in hydrogen bonds and the role of hydrogen bonding in azo aggregation has been established [2].

Table 2. ^{1}H NMR and ^{13}C NMR spectral data of 5-(4′-nitrophenylazo)-8-hydroxyquinolin (HL_5).

Group* (number)	^{1}H NMR δ, ppm (H atoms, peak, assignment)	^{13}C NMR δ, ppm (H atoms, peak, assignment)
02	9.30	146.92
04	8.66	135.99
10	–	129.73
09	–	128.70
06	8.25	123.45
07	7.01	111.50
08	–	147.06
OH	10.30	–
05	–	137.10
11	–	157.66
12	7.87	121.24
13	8.25	125.04
14	–	157.66
15	8.25	125.04
16	7.87	121.24

*See figure 4 for numbers.

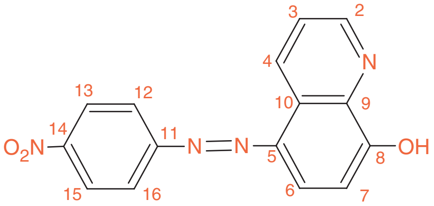

Figure 4. Structure of 5-(4-nitrophenylazo)-8-hydroxyquinoline (HL_5).

3.3. ^{1}H NMR spectra

The ^{1}H and ^{13}C NMR spectra of (HLn) were recorded in dimethylsulphoxide (DMSO-d_6) solution using tetramethylsilane (TMS) as internal standard.

Mubarak, El-Sonbati and coworkers [14–26] investigated the NMR spectra of quinoline and its derivatives with various transition metal salts. The ^{1}H NMR spectra (table 2 and figure 4) show signals for C_8–OH (9.52–10.30) and HCN (8.89–9.28) ppm, favoring formation of an intramolecular hydrogen bond with the azomethine group. Electron-withdrawing substituents reduce the intramolecular hydrogen bond as indicated by the marked shift of the hydroxyl signal to higher field in the p-NO_2 and p-Cl compounds. Electron-donating substituents give the opposite effect, arising from the increasing basicity of the azo-nitrogen. The broad signals due to the C_8–OH protons at 9.52–10.30 ppm are not affected by dilution but rapidly exchange in the presence of D_2O. According to Mubarak, El-Sonbati and coworkers [14–26], hydrogen bonding leads to a large deshielding of these protons. Signals in the range 7.00–8.66 ppm correspond to aromatic protons (the integration curve show 15 protons except for HL_1 and HL_2 which show 16 protons). For the HL_1 a singlet observed at 2.36 ppm is assigned to CH_3 protons (the integration curve shows 3 protons). Also HL_2 has a singlet at 3.76 ppm which is assigned to the OCH_3 protons. The shifts are observed in the sequence: p-$NO_2 > p$-$Cl > p$-$H > p$-$OCH_3 > p$-CH_3.

The ^{13}C NMR spectral data of (HL_5) (table 2 and figure 4) confirms the result of the ^1H NMR spectrum of the ligand (HL_5).

3.4. *Infrared spectra and nature of coordination*

The interaction of azo compounds, R–N=N–R, with transition metal salts produced complexes of at least four different types:

(a) the azo compound attached *via* nitrogen α-donor bonds;
(b) azo compound bonded *via* π-bonds involving the π-electrons of the –N=N– system;
(c) a metalated ligand attached *via* one nitrogen and a metal-carbon σ-bond to the ortho carbon of the ring for aromatic derivatives;
(d) a rearranged nitrogen-donor, e.g. *o*-semidine azobenzene acts as a fairly strong π-acid.

Comparison of infrared spectra of free ligands and their Ru^{+3} complexes indicate that these ligands are monobasic bidentate where Ru^{+3} is coordinated through metal-chelate rings in an N,N:O (N,N:O) trans geometry [10, 14–26]. The HLn ($n = 1$–5) ligands were obtained in good yield.

The *bis*-[5-(4′-*R*-phenylazo)-8-hydroxyquinoline] reacts with $RuCl_3$ (molar ratio 1 : 1 in ethanol) giving solid, dark brown or red complexes with the expected $[Ru(Ln)Cl_2 \cdot OH_2]_2$ stoichiometry deduced from elemental analyses (table 1 and figure 5).

Important structural IR bands like ν(C–O), ν(C=N), ν(–N=N–), ν(Ru–O) and ν(Ru-N) have been assigned throwing light on the structural features of the new azodye ligand and its mode of bonding to the metal ions. Broad bands at 3450, 2109 and 925 cm^{-1} are assigned to OH and hydrogen bonds. Mubarak and El-Sonbati [14–26] found three kinds of bonded OH structures on the basis of the IR frequencies:

(i) Only oxygen is in the bridge while the hydrogen is free.
(ii) Polymer chains are formed in which both hydrogen and oxygen atoms participate in the hydrogen bond.
(iii) Dimer associated structures are formed.

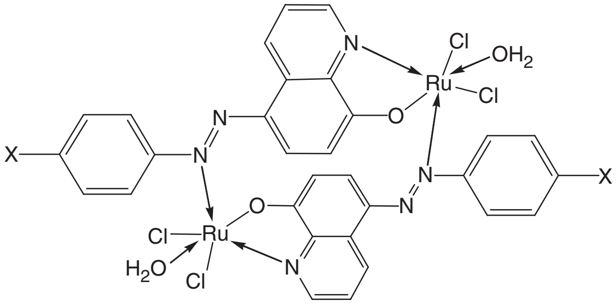

Figure 5. Structure of *bis*-[5-(4′-*R*-phenylazo)-8-hydroxyquinoline] ruthenium.

HLn exists as a five-membered chelate skeleton with hydrogen bonding classified into two types:

(a) An intramolecular hydrogen bond O–H$\cdots$N (figure 3a) is found between hydrogen of (C_8-OH) and nitrogen of azomethine group (CN_{Py}).
(b) An intermolecular hydrogen bonding O–H$\cdots$N (figure 3b) and (O–H$\cdots$O) (figure 3c) resulting from the C_8–OH group itself and/or C_8–OH with CN between two molecules. The strong 950 cm^{-1} band indicates the existence of this ligand in a dimer skeleton, associated structure through intermolecular hydrogen bonds.

The ligands are likely coordinated in a tridentate fashion *via* N=N, CN and OH of quinoline with displacement of a proton from the latter group. This is supported by disappearance of ν(OH) of quinoline and appearance of a new band at ~1350 cm^{-1}, ν(C–O) (~1340 cm^{-1} in ligands) in metal chelates, indicating deprotonation of phenolic hydroxyl groups and monobasic nature of the ligand in complexes indicating coordination through the oxygen atom of the phenol group. This is further supported by the appearance of the band at 460–510 cm^{-1} due to metal-oxygen stretching in the complexes. The strong ligand azo group bands at 1450 and 1425 cm^{-1} are shifted from their positions by about 15 cm^{-1} indicating coordination through one of the nitrogen atoms of the azo group. Consequently, the azo group is involved in coordination with Ru^{3+}. The pyridine ν(C=N) (1580–1570 cm^{-1}) is characterized by a very strong band, which, upon complexation, shifted to lower frequency with a reduction in its intensity indicating coordination of the azomethine nitrogen. This is further supported by the appearance of the band corresponding to the metal-nitrogen stretching vibration at 590–610 cm^{-1} in the spectra of complexes [2, 14–18, 33]. Furthermore, δ_{Py} appeared at ~640 cm^{-1} in the free ligands, exhibiting a negative shift in the complexes indicating that the pyridine ring is involved in coordination through its CN donor.

The mode of coordination is also confirmed from the NMR data in which the OH signal disappeared. This is accompanied by disappearance of the hydrogen bond and displacement of a proton as well as the coordination through the oxygen of hydroxyl.

3.5. *Magnetic moments*

The magnetic susceptibility measurements lie between 1.73 and 1.94 B.M. indicating the presence of one unpaired electron. It is inferred from the values that ruthenium is in the +3 oxidation state.

3.6. *Electronic spectra*

HLn exhibited bands at 32,500–32,150 cm^{-1} (CN) (π–π*), 33,450–33,340 cm^{-1} (H-bonding and association), 40,038–39,460 cm^{-1} (phenyl) (Ph–Ph*, π–π*) [17] and 29,340–29,230 cm^{-1} transition of phenyl rings overlapped by composite broad (π–π*) of azo structure. The band due to the $n \rightarrow \pi^*$ transition is associated mainly with the color of the compound [2, 15]. The donor substitutents cause a red shift relative to the unsubstituted derivative (H) in the order $OCH_3 > CH_3 > H > Cl > NO_2$, the *x*-phenyl moiety acts as an electron donor center while the C=N group acts as an electron acceptor. Thus these compounds behave as donor–acceptor conjugated systems and the

CT takes place between these two centers [4]. The analytical data (table 1) and the spectral properties of the ligands are consistent with their structure in figure 3.

3.7. *ESR measurements*

The geometry of the Ru^{+3}-azodye complexes was further confirmed by ESR spectra which gives insight into the spatial distribution of the ligand groups around the central metal ion indicates possible metal–metal interactions in the solid state. The spectra of complexes show no interaction between rutheniums in complexes **1**–**5**. For the investigated x-band ESR spectra of the powdered complexes, at room temperature, a positive contribution to the g value is increasing in the order: complex $1(2.142) > 2(2.056) > 3(2.045) > 4(2.032) > 5(2.018)$. Accordingly, the g values of the studied complexes depend on the substituent effect of the aromatic ring i.e., affected by the charge density on the chelating ring. As can be seen from figure 6, the plot of g values *versus* σ [σ = Hammet's constant of R] is linear.

3.8. *UV–Vis spectra and geometry of the complexes*

Ruthenium(III) in octahedral environment (t_{2g}^5) is $^2T_{2g}$ in accord with the magnetic moment values in table 3. The first excited doublet levels will be $^2A_{2g}$ and $^2T_{1g}$. The energy difference between these two states ($^2T_{2g}$ and $^2A_{2g}$) is ($10Dq - 3F_2 - 20F_4$) [25, 26] assuming pure quantization.

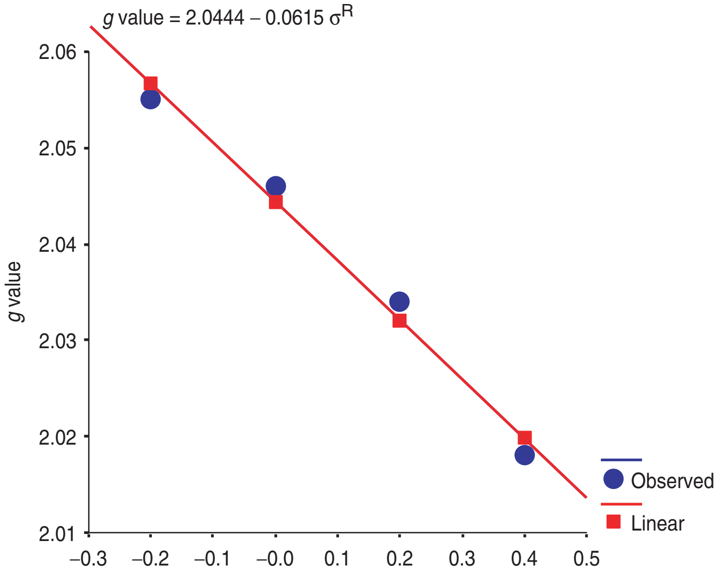

Figure 6. The variation of p-substituted Hammet's constant (σ^R) [σ = Hammet's constant of R] with g values.

The geometry in the Ru^{+3}-azodye complexes under investigation was studied by electronic absorption spectra, magnetic moment determination and ESR measurements.

The electronic absorption spectra of Ru^{+3}-azodye complexes under study show three groups of bands. The absorption bands are in the same pattern through appearing with varied extinction and changed absorption maxima which can be ascribed to changes in the molecular structure of the ligands leading to varied strength in the azodye → Ru^{+3} interaction. Of the three regions, the bands with frequencies above 35,000 cm^{-1} can be assigned to localized π–π^* transitions of the aromatic system. The bands within 20,000–35,000 cm^{-1} represent various types of c.t. interactions either within the ligand molecule (intraligand c.t.) or due to $L \rightarrow Ru^{3+}$ or $Ru^{3+} \rightarrow L$ c.t. interactions.

The third group of bands lying below 20,000 cm^{-1} usually exhibits three distinct peaks. These three peaks can be attributed to three spin forbidden d–d transitions at ca 13,333–14,388 $[^2T_{2g} \rightarrow {}^4T_{1g}]$, 16,949–18,181 $[^2T_{2g} \rightarrow {}^4T_{2g}]$ and 19,234–19,810 cm^{-1} $[^2T_{2g} \rightarrow {}^2A_{2g}, {}^2T_{1g}]$ as expected for octahedral symmetry of low spin Ru(III) complexes [24–26]. The separation between the two low energy spin-forbidden transitions $^2T_{2g} \rightarrow {}^4T_{1g}$ and $^2T_{2g} \rightarrow {}^4T_{2g}$, corresponds to 8B [24–26]. The magnitude of this separation is useful in calculation the value of 10Dq from the electronic repulsion parameter *B*.

The electronic spectra may be further rationalized in terms of ligand field parameters (table 3), which show that the values of the Racah parameter *B* are less than the free ion value, an indication of strong covalent bonding between the metal ion and the ligand. The effect of covalent bonding is reflected by the high value of 10 Dq. Such a value is generally associated with considerable electron delocalization [24–26].

The nephelauxetic parameter, β, is in the 0.58–0.68 range indicating that HL_n is in the middle nitrogen and oxygen donor series. It is apparent that the parameter, β, depends on the electronegativity of the donor atom and the ligand structure. According to Jørgensen [34], decreasing values of *B* are associated with a reduction in the effective positive charge of the metal ion and an increasing tendency to reduction to the next

Table 3. Electronic absorption spectra, ligand field parameters (cm^{-1}) and g values of Ru^{3+}-azodye complexes (for molecular structure see figure 5).

Complex[a]	Bands (obs.)	ν_2/ν_1	Dq	*B*	β	*C*	F_2	F_4	Z^*	*g* values
1	14030 18230 18485	1.30	2505.5	525	0.68	2100	825	60.0	1.4	2.142
2	14180 18295 19350	1.29	2497.8	515	0.65	2060	809	58.9	1.3	2.056
3	14333 18360 19900	1.28	2490.0	503	0.63	2012	790	57.5	1.3	2.045
4	14280 18200 20250	1.28	2457.0	490	0.60	1960	770	56.0	1.2	2.032
5	13999 17880 19880	1.28	2418.4	485	0.58	1940	762	55.4	1.4	2.018

[a] The number corresponds to that used in table 1 and figure 5.

lower oxidation state. For 4d metals, the variation in the Racah interelectronic repulsion parameters with the ionic charge, Z*, and the number of electrons in the partially filled d-state (q) is given by the equation:

$$B = 742 + 28q + 50(Z^* + 1) - \frac{500}{(Z^* + 1)}$$

The Z^*-values of the ruthenium(III) in the complexes, listed in table 3, lie in the 1.2–1.4 range, considerably below the formal value of +3 oxidation state.

As can be seen from table 3, the Racah parameters (Dq, B, β) and C, F_2 and F_4 values increased from compound **5** to **1**. This can be attributed to the effective charge experienced by the d-electrons decreasing due to the electron withdrawing *p*-substituent (HL_4 and HL_5) and increasing the electron-donating character of HL_1 and HL_2. As can be seen from table 1, the yield of compounds decreases from withdrawing to donating *p*-position, in accord with expectations from Hammet's constant (σ^R) (figure 7).

The above results show clearly the effect of substituents in the *para* position of the benzene ring on the stereochemistry of Ru^{3+} complexes. The existence of a methyl and/or methoxy group enhances the electron density on the coordination sites and increases the values of Racah parameters (table 3).

3.9. *Thermal analysis*

The thermal analyses of ruthenium complexes under study were carried out in an attempt to clarify the content and bonding of water in the complexes.

The TG analyses display three regions of change, which are almost common for all the complexes. The first region characterizes removal of water at 160°C. The second and third steps characterize dechlorination within the temperature range 220–350°C. In this region the differential thermal analysis showed mixed endothermic-exothermic character, denoting elimination of the chloride ions (endothermic process) and a partial ignition of the organic ligand (exothermic process). The dechlorinated complexes then decompose to metal oxide in the temperature range 350–700°C. The values of ruthenium content, determined from the remaining oxide, were found to be in satisfactory agreement with the values calculated on the basis of the suggested composition formula obtained from data of elemental analysis.

4. Conclusion

(1) All complexes are stable on heating to 200°C. The first decomposition step may be attributed to removal of one water molecule followed by removal of two chloride molecules and then the ligand.

(2) The azodye derivatives are tridentate ligands, coordinating *via* N=N, C=N and OH groups as shown in figure 5, on the basis of IR. The IR spectra of the complexes reveal participation of (C–O) group coordinated with the Ru^{3+} ion. HL_n is a

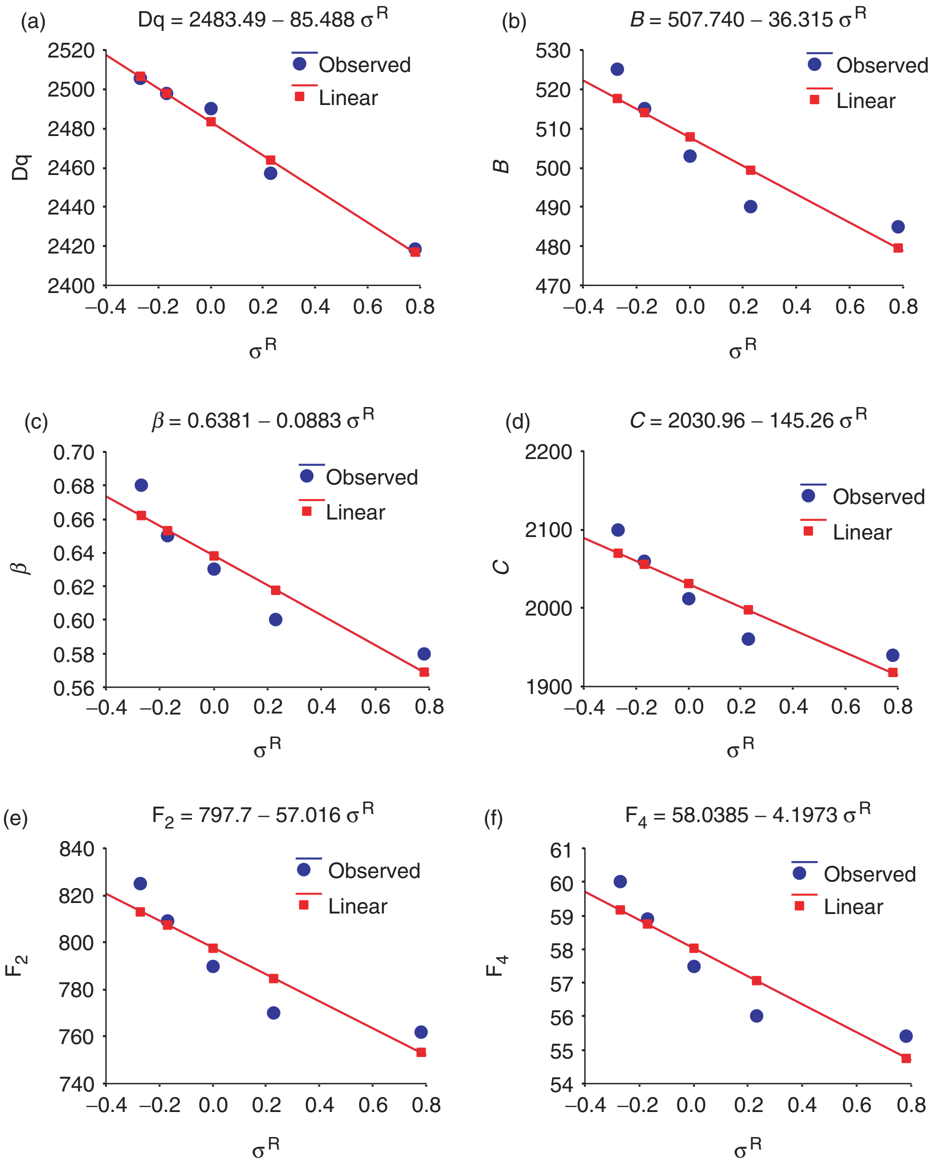

Figure 7. The variation of *p*-substituted Hammet's constant (σ^R) [σ = Hammet's constant of *R*] with: (a) Dq, (b) B, (c) β, (d) C, (e) F_2 and (f) F_4.

mononegative tridentate ligand *via* OH group (^{1}H NMR and IR spectra) forming a five-membered ring as shown in figure 5.

(3) The coordination behaviour of the nitrogen of (N=N) and OH_2 groups confirm the stability of metal ion in the ring. The stability of the complexes also depends on the number of donating atoms in the ring and upon the nature of the transition metal.
(4) Based on Hammet's relationship, electron-withdrawing substituents to ligands in their complexes enhance the stabilities of these complexes owing to the decrease of electron density at the metal atom and thus increase the positive charge on

the metal. This effect results in decreasing reactivity. In contrast, electron-donating substituents increase the electron density at the metal, leading to decreased stability of the metal chelates.

(5) Previous studies [14–16, 22, 26, 33] investigated the effect of substituents on the stabilities of complexes showing a linear relationship between values of the Racah parameter and the *p*-substituent Hammet constant σ^R with negative slope, i.e the higher the value of σ^R (stronger electron withdrawal) the lower values of the Racah parameter, and the higher the stability. Accordingly, the Racah parameter values decrease and thus the stability of the complexes increase in the following order: p-$NO_2 > p$-$Cl > p$-$H > p$-$CH_3 > p$-OCH_3.

(6) The magnetic results for all complexes indicate low-spin t_{2g}^5 Ru^{3+} in an octahedral environment.

References

[1] W.I. Jorgensen, J. Pranata. *J. Am. Chem. Soc*., **112**, 2008 (1990).
[2] A.T. Mubarak. *Spectrochim. Acta Part A*, **65**, 1197 (2006); *J. Coord. Chem*., **60**, 1771 (2007).
[3] A.T. Mubarak, A.Z. El-Sonbati. *Polym. Bull*., **57**, 683 (2006).
[4] M. Albrecht, O. Blau, R. Frohlich. *Chem. Eur. J*., **5**, 48 (1999).
[5] M. Albrecht, E. Wegehus, O. Blau, K. Rissanen. *New J. Chem*., **23**, 667 (1999).
[6] E. Proffit, G. Buchmann. *Arznemittel Forsch*, **10**, 181 (1960).
[7] H. La Roche. Swiss Patent, 416648 (1967).
[8] J.A. Vaichulis, US Patent, 3272352 (1966).
[9] H. Dietrich, Swiss Patent, 454874 (1968).
[10] L.H. Schmidt. *Ann. Rev. Microbiol*., **427**, 23 (1969).
[11] S. Aktiesel, F. Kabet. Dan. Patent, 108626 (1968).
[12] C. Tommos, G.T. Babcock. *Acc. Chem. Res*., **31**, 18 (1998).
[13] M. Kasha. *J. Chem. Soc*., **82**, 2379 (1986).
[14] A.T. Mubarak. *Spectrochim. Acta Part A*, **61**, 1163 (2005).
[15] A.T. Mubarak. *Design. Mon. Polym*., **8**, 1 (2005).
[16] A. El-Dissouky, A.Z. El-Sonbati. *Trans. Met. Chem*., **11**, 112 (1986).
[17] A.Z. El-Sonbati, A, El-Dissouky. *Trans. Met. Chem*., **12**, 256 (1987).
[18] A.Z. El-Sonbati. *Spectrosc. Lett*., **30**, 459 (1997).
[19] A.A. El-Bindary, A.Z. El-Sonbati. *Gazz. Chim. Ital*., **127**, 597 (1997).
[20] A.Z. El-Sonbati, A.A. El-Bindary. *Pol. J. Chem*., **74**, 621 (2000).
[21] A.A. El-Bindary, A.Z. El-Sonbati. *Pol. J. Chem*., **74**, 615 (2000).
[22] A.F. Shoair, A.A. El-Bindary, A.Z. El-Sonbati, R.M. Younes. *Spectrochim. Acta Part A*, **57**, 1683 (2001).
[23] A.Z. El-Sonbati, A.A. El-Bindary, A.F. Shoair, R.M. Younes. *Chem. Pharm. Bull*., **49**, 1308 (2001).
[24] A.Z. El-Sonbati, A.A. El-Bindary, A.A. El-Sarawy. *Spectrochim. Acta Part A*, **58**, 2771 (2002).
[25] A.Z. El-Sonbati, A.A. El-Bindary, A.F. Shoair. *Spectrochim. Acta Part A*, **58**, 3003 (2002).
[26] A.T. Mubarak, S.A. El-Assiery. *Appl. Organometal. Chem*., **18**, 343 (2004).
[27] E. Bardez, I. Devol, B. Larry, B. Valeur. *J. Phys. Chem. B*, **101**, 7786 (1997).
[28] I. Suryanarayana, B.K. Saikia. *J. Pure Appl. Phys*., **18**, 1010 (1980).
[29] A.T. Mubarak, A.Z. El-Sonbati, A.A. El-Bindary. *Chem. Pap*., **58**, 320 (2004).
[30] A. Yonda, T. Hakushi, G.R. Newkome, T. Matsmshita. *Acta Crystallogr. Sect. C*., **52**, 172 (1996).
[31] S. Millifiori, G. Favini. *Z. Phys. Chem*., **75**, 23 (1971).
[32] H.H. Jaffe, S.J. Yeh, R.W. Gardner. *J. Mol. Spectrosc*., **2**, 120 (1958).
[33] A.T. Mubarak, A.Z. El-Sonbati, A.A. El-Bindary. *Appl. Organometal. Chem*., **18**, 212 (2004).
[34] C.K. Jørgensen. *Helv. Chem. Acta*, **56**, 131 (1967).